



**HAL**  
open science

## Reliable non-linear state estimation involving time uncertainties

Simon Rohou, Luc Jaulin, Lyudmila Mihaylova, Fabrice Le Bars, Sandor M Veres

► **To cite this version:**

Simon Rohou, Luc Jaulin, Lyudmila Mihaylova, Fabrice Le Bars, Sandor M Veres. Reliable non-linear state estimation involving time uncertainties. *Automatica*, 2018, 93, pp.379-388. 10.1016/j.automatica.2018.03.074 . hal-01778187

**HAL Id: hal-01778187**

**<https://hal.science/hal-01778187v1>**

Submitted on 25 Apr 2018

**HAL** is a multi-disciplinary open access archive for the deposit and dissemination of scientific research documents, whether they are published or not. The documents may come from teaching and research institutions in France or abroad, or from public or private research centers.

L'archive ouverte pluridisciplinaire **HAL**, est destinée au dépôt et à la diffusion de documents scientifiques de niveau recherche, publiés ou non, émanant des établissements d'enseignement et de recherche français ou étrangers, des laboratoires publics ou privés.

# Reliable Non-Linear State Estimation Involving Time Uncertainties

Simon Rohou<sup>a</sup>, Luc Jaulin<sup>a</sup>, Lyudmila Mihaylova<sup>b</sup>, Fabrice Le Bars<sup>a</sup>,  
Sandor M. Veres<sup>b</sup>

<sup>a</sup>ENSTA Bretagne, Lab-STICC, UMR CNRS 6285, Brest, France

<sup>b</sup>The University of Sheffield, Department of Automatic Control and Systems Engineering, Sheffield, United Kingdom

---

## Abstract

This paper presents a new approach to bounded-error state estimation involving time uncertainties. For a given bounded observation of a continuous-time non-linear system, it is assumed that neither the values of the observed data nor their acquisition instants are known exactly. For systems described by state-space equations, we prove theoretically and demonstrate by simulations that the proposed constraint propagation approach enables the computation of bounding sets for the systems' state vectors that are consistent with the uncertain measurements. The bounding property of the method is guaranteed even if the system is strongly non-linear. Compared with other existing constraint propagation approaches, the originality of the method stems from our definition and use of bounding tubes which enable to enclose the set of all feasible trajectories inside sets. This method makes it possible to build specific operators for the propagation of time uncertainties through the whole trajectory. The efficiency of the approach is illustrated on two examples: the dynamic localization of a mobile robot and the correction of a drifting clock.

*Key words:* state estimation, time uncertainties, non-linear systems, tubes, robotics, constraints, contractors

---

## 1 Introduction

This paper presents a novel method for the state estimation of a dynamical system of the form:

$$\begin{cases} \dot{\mathbf{x}}(t) = \mathbf{f}(\mathbf{x}(t), \mathbf{u}(t)), & (1a) \\ z_i = g(\mathbf{x}(t_i)), & (1b) \end{cases}$$

where  $\mathbf{x}(t) \in \mathbb{R}^n$  is the state vector representing the system at time  $t$  and  $\mathbf{f} : \mathbb{R}^n \times \mathbb{R}^m \rightarrow \mathbb{R}^n$  a non-linear function depicting the evolution of the system based on input vectors  $\mathbf{u}(t) \in \mathbb{R}^m$ . The observation function  $g : \mathbb{R}^n \rightarrow \mathbb{R}$  is assumed to be scalar, without loss of generality as the methods are readily scalable to the vector case. The  $t_i$ ,  $i \in \mathbb{N}$ , are measurement times and the  $z_i$  are the related outputs.

In a bounded-error approach to the state estimation problem, we can assume the function  $\mathbf{f}$  and the measurements  $z_i$  are not known exactly. Instead, we shall consider that  $\mathbf{f}$  is represented by a set-valued function [f]

and that measurements  $z_i$  all belong to some known intervals denoted by  $[z_i]$ . When the  $t_i$  are exactly known, interval analysis [21] combined with constraint propagation [4, 14] is able to efficiently solve the state estimation problem [20, 15, 24]. More precisely, without any prior knowledge on the state, an interval calculus allows to compute for each  $t$  a set enclosing all feasible state vectors.

This paper deals with uncertain measurement times: the  $t_i$  are only known to belong to some interval  $[t_i]$ . In this context, neither the value of the output  $z_i$  nor the acquisition date  $t_i$  are known exactly. Hence, the problem becomes much more complex as the uncertainties related to the  $t_i$  are difficult to propagate through the differential equation. Some attempts of using interval analysis have been proposed in [5, 18], but the corresponding observers cannot be considered as guaranteed. Other works, often referred as Out Of Sequence Measurement (OOSM) [9], state problems of time delay uncertainties, which can be somehow related to our problem. However, the considered time uncertainties are tight, of the same order of magnitude as computational time step, and treated by means of covariance matrices which do not provide guar-

---

\* Corresponding author: simon.rohou@ensta-bretagne.org

anted results. In contrast, this paper proposes a reliable computational tool set to deal with strong temporal uncertainty constraints in systems involving differential equations and non-linear functions.

**Motivating application.** Some practical problems can be formulated to deal with time uncertainties. As an illustration, let us consider an underwater robot  $\mathcal{R}$  performing an exploration task using a side-scan sonar. Assume that a localization of the robot is based on the perception of a wreck for which the highest point  $\mathbf{w}$  is precisely geolocalized. As pictured in Figure 1, the wreck image  $\mathbb{W}(t)$  obtained by the sonar may be distorted, stretched and would be highly noisy in practice, depending on the robot navigation [18]. It is a difficult problem for image processing algorithms to detect the highest point  $\mathbf{w}$  in  $\mathbb{W}$  to be used as reference for localization. However, the problem can be dealt with in a temporal way, based on the time interval  $[t]$  during which the robot has seen the wreck. This observation is related to a strong temporal uncertainty: up to several seconds or minutes. Then the state estimation amounts to a range-only problem for which  $\exists t \in [t], \exists \rho \in [\rho] \mid \rho = g(\mathbf{x}(t))$ , with  $g: \mathbb{R}^n \rightarrow \mathbb{R}$  the distance function between  $\mathcal{R}$  and the known point  $\mathbf{w}$ .

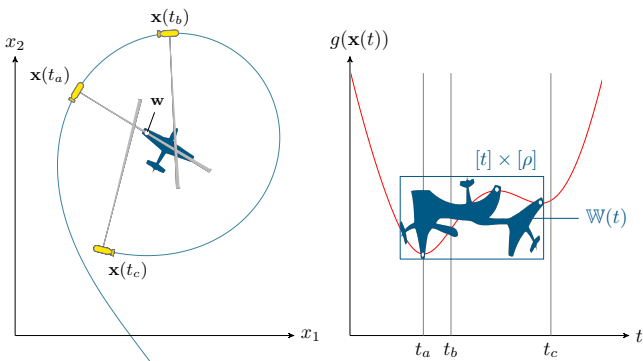


Fig. 1. A robot  $\mathcal{R}$  perceiving a plane wreck by using a side scan sonar. The observation function  $g(\mathbf{x})$  represents the distance between  $\mathcal{R}$  and a point of interest  $\mathbf{w}$  on the plane, pictured by a white dot and seen at times  $t_1 = t_a, t_2, t_3$ . The sonar image  $\mathbb{W}(t)$  is overlaid on the graph. Although  $\mathbf{w}$  has been seen three times, the  $t_i$  remain uncertain but known to belong to  $[t]$ . Some other robot states are illustrated at times  $t_a, t_b, t_c$ .

This example shows how a classic robotic application can be related to strong time uncertainties. The current paper is a first step towards new state estimation approaches that will focus on both the time and the state spaces. It proposes a theoretical basis to deal with the former in the most generic way and is illustrated by reproducible examples in order to highlight the interest and simplicity of the method and encourage further comparisons.

This paper is organized as follows. Section 2 gives an

overview of constraint propagations related to sets of trajectories, introducing the concept of Constraint Networks, tubes and contractors. These tools will then be extended to the time uncertainty constraint this paper is dealing with. The approach, theoretically detailed in Section 3, will be illustrated through two robotics examples. The first one, Section 4, involves a mobile robot to be localized while evolving amongst beacons emitting uncertain range-only signals. The second one, detailed in Section 5, provides an original method to correct a drifting clock using ephemeris measurements. Sections 6 and 7 conclude the paper and present the numerical libraries used during this work.

## 2 Constraint propagation over trajectories

Subsection 2.1 recalls the principle of constraint propagation [27, 4] that will be used later to formalize problems concerning dynamical systems. To this end, a *tube* can be used to enclose a feasible solution set: an envelope of trajectories compliant with the selected constraints. The notion of tube is recalled in Subsection 2.2 with related properties.

### 2.1 Constraint Networks

In a numerical context, problems of control, state estimation and robotics can be described as *Constraint Networks* (CNs), in which variables must satisfy a set of rules or facts, called *constraints*, over domains defining a range of feasible values. Links between the constraints define a network [19] involving variables  $\{x_1, \dots, x_n\}$ , constraints  $\{\mathcal{L}_1, \dots, \mathcal{L}_m\}$  and domains  $\{\mathbb{X}_1, \dots, \mathbb{X}_n\}$  containing the  $x_i$ 's. The variables  $x_i$  can be symbols, real numbers [3] or vectors of  $\mathbb{R}^n$ . The constraints can be non-linear equations between the variables, such as  $x_3 = \cos(x_1 + \exp(x_2))$ . Domains can be intervals, boxes [16], or polytopes [10].

**Contractors.** A constraint  $\mathcal{L}$  can be applied on a box  $[\mathbf{x}] \in \mathbb{I}\mathbb{R}^n$  with the help of a contractor  $\mathcal{C}$ . The box  $[\mathbf{x}]$ , also called *interval-vector*, is a closed and connected subset of  $\mathbb{R}^n$  and belongs to the set of  $n$ -dimensional boxes denoted by  $\mathbb{I}\mathbb{R}^n$ . Formally, a contractor  $\mathcal{C}$  associated to the constraint  $\mathcal{L}$  is an operator  $\mathbb{I}\mathbb{R}^n \rightarrow \mathbb{I}\mathbb{R}^n$  that returns a box  $\mathcal{C}([\mathbf{x}]) \subseteq [\mathbf{x}]$  without removing any vector consistent with  $\mathcal{L}$ . Constructing a store of contractors such as  $\mathcal{C}_+, \mathcal{C}_{\sin}, \mathcal{C}_{\exp}$  associated to primitive equations such as  $z = x + y, y = \sin(x), y = \exp(x)$  has been the subject of much work [16, 8, 11].

**Decomposition.** Problems involving complex equations can be broken down into a set of primitive equations. Here, *primitive* means that the constraint cannot be decomposed anymore and that the related operator is available in a collection of contractors, thus allowing to deal with a wide range of problems. For instance,

the non-linear equation  $x_3 = \cos(x_1 + \exp(x_2))$  can be decomposed into:

$$\begin{cases} a = \exp(x_2), \\ b = x_1 + a, \\ x_3 = \cos(b). \end{cases} \quad (2)$$

Combining primitive contractors leads to a complex contractor that still provides reliable results [8].

**Propagation.** When working with finite domains, a propagation technique can be used to solve a problem. The process is run up to a fixed point when domains  $\mathbb{X}_i$  cannot be reduced anymore.

Our goal is to consider trajectories as variables and to implement contractors to reduce their domains given a constraint that can be algebraic or differential. This will be done by using tubes as domains for these variables.

## 2.2 Tubes: envelopes of feasible trajectories

In this paper, the notation  $(\cdot)$  is used in order to clearly distinguish a whole trajectory  $\mathbf{x}(\cdot) : \mathbb{R} \rightarrow \mathbb{R}^n$  from a local evaluation:  $\mathbf{x}(t) \in \mathbb{R}^n$ .

**Definition.** A tube is defined [17, 13] over a domain  $[t_0, t_f]$  as an envelope enclosing an uncertain trajectory  $\mathbf{x}(\cdot)$ . We will use the definition given in [18, 6] where a tube  $[x](\cdot) : \mathbb{R} \rightarrow \mathbb{I}\mathbb{R}^n$  is an interval of two trajectories  $[x^-(\cdot), x^+(\cdot)]$  such that  $\forall t, x^-(t) \leq x^+(t)$ . A trajectory  $x(\cdot)$  belongs to the tube  $[x](\cdot)$  if  $\forall t, x(t) \in [x](t)$ . Figure 2 illustrates a scalar tube enclosing a trajectory  $x^*(\cdot)$ . For the sake of simplicity, the following tubes mentioned in Sections 2.2–3.1 will be of dimension 1, without loss of generality.

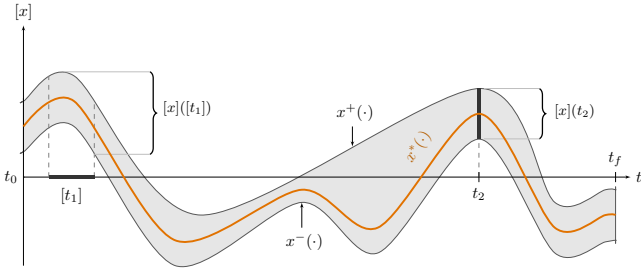


Fig. 2. A tube  $[x](\cdot)$ , interval of two functions  $[x^-(\cdot), x^+(\cdot)]$ , enclosing a random signal  $x^*(\cdot)$ .

It is possible to implement a tube in several ways. A computer representation based on a set of boxes that sample the tube over time has been mentioned in [18, 6, 26].

**Arithmetics.** Consider two tubes  $[x](\cdot)$  and  $[y](\cdot)$  and an operator  $\diamond \in \{+, -, \cdot, /\}$ . We define  $[x](\cdot) \diamond [y](\cdot)$  as

the smallest tube (with respect to inclusion) containing all feasible values for  $x(\cdot) \diamond y(\cdot)$ , assuming that  $x(\cdot) \in [x](\cdot)$  and  $y(\cdot) \in [y](\cdot)$ . This definition is an extension to trajectories of the interval arithmetic proposed by Moore [22]. If  $f$  is an elementary function such as  $\sin, \cos, \dots$ , we define  $f([x](\cdot))$  as the smallest tube containing all feasible values for  $f(x(\cdot))$ ,  $x(\cdot) \in [x](\cdot)$ .

Figures 3a–3b present two scalar tubes  $[x](\cdot)$  and  $[y](\cdot)$ . The tube arithmetic makes it possible to compute any algebraic operation on tubes, as illustrated by Figures 3c–3f.

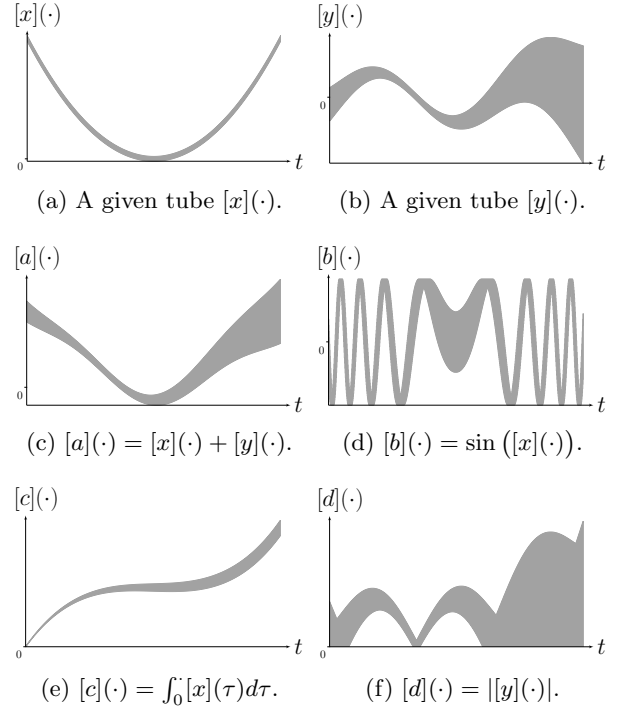


Fig. 3. Tube arithmetics. Note that the vertical scales of these figures vary for full display.

## 2.3 Contractors for tubes

The contractors recalled in Subsection 2.1 can be extended to sets of trajectories, thus allowing constraints over time such as  $a(\cdot) = x(\cdot) + y(\cdot)$  or  $b(\cdot) = \sin(x(\cdot))$ . A *tube contractor* has been defined in [6] and is recalled here.

**Definition 1** A contractor  $\mathcal{C}_{\mathcal{L}}$  applied on a tube  $[x](\cdot)$  aims at removing infeasible trajectories according to a given constraint  $\mathcal{L}$  so that:

- (i)  $\mathcal{C}_{\mathcal{L}}([x](\cdot)) \subseteq [x](\cdot)$ , (contraction)
- (ii)  $\left( \begin{array}{l} \mathcal{L}(x(\cdot)) \\ x(\cdot) \in [x](\cdot) \end{array} \right) \Rightarrow x(\cdot) \in \mathcal{C}_{\mathcal{L}}([x](\cdot))$ . (consistency)

For instance, the minimal contractor  $\mathcal{C}_+$  associated with the constraint  $a(\cdot) = x(\cdot) + y(\cdot)$  is:

$$\begin{pmatrix} [a](\cdot) \\ [x](\cdot) \\ [y](\cdot) \end{pmatrix} \mapsto \begin{pmatrix} [a](\cdot) \cap ([x](\cdot) + [y](\cdot)) \\ [x](\cdot) \cap ([a](\cdot) - [y](\cdot)) \\ [y](\cdot) \cap ([a](\cdot) - [x](\cdot)) \end{pmatrix}. \quad (3)$$

In this way, information on either  $[a](\cdot)$ ,  $[x](\cdot)$  or  $[y](\cdot)$  can be propagated to the other tubes.

**Differential contractor.** The primitive constraint relying on the differential equation  $\dot{x}(\cdot) = v(\cdot)$  has been the subject of [26], introducing the contractor  $\mathcal{C}_{\frac{d}{dt}}([x](\cdot), [v](\cdot))$  that will contract the tube  $[x](\cdot)$  from its derivative bounded by  $[v](\cdot)$ .  $\mathcal{C}_{\frac{d}{dt}}$  is of interest to propagate some local evaluation  $z = x(t)$ ,  $z \in [z]$ ,  $x(\cdot) \in [x](\cdot)$  over the whole tube domain. However, it does not apply when  $t$  is not known exactly. This motivates the study of a new primitive contractor to apply any uncertain tube evaluation.

When the derivative not only depends on time but also on the trajectory itself, as for dynamical systems described by Eq. (1a), a decomposition is used to reduce the problem to a set of simple constraints. For instance,  $\dot{\mathbf{x}}(\cdot) = \mathbf{f}(\mathbf{x}(\cdot))$  will be broken down into  $\dot{\mathbf{x}}(\cdot) = \mathbf{v}(\cdot)$  and  $\mathbf{v}(\cdot) = \mathbf{f}(\mathbf{x}(\cdot))$  where  $\mathbf{f}$  is a set of algebraic constraints. Then, an iterative resolution will apply to propagate information between  $\mathbf{x}(\cdot)$  and  $\mathbf{v}(\cdot)$  till a fixed point is reached. This allows to deal with general dynamical systems. However, as stated in [26], the proposed approach may be too pessimistic when a cyclic differential constraint is encountered, such as  $\dot{x} = -\sin(x)$ . In such case, a combination with other approaches such as CAPD [28] or DynIBEX [1] has to be studied.

### 3 Generic contractor for trajectory evaluation

This section provides a reliable tool to deal with any uncertain evaluation  $z$  of a trajectory  $y(\cdot)$  at a given time  $t$ . This is formalized by a primitive constraint denoted  $\mathcal{L}_{\text{eval}} : z = y(t)$ , which is a fundamental issue in the field of CNs involving dynamical systems. Here, the trajectory  $y(\cdot)$ , its derivative  $w(\cdot)$ , the observation time  $t \in \mathbb{R}$  and the measurement  $z \in \mathbb{R}$  are all known to belong to respective domains. Our contribution is to propose a new contractor  $\mathcal{C}_{\text{eval}}$  that will optimally reduce these bounds by removing solutions not compliant with  $\mathcal{L}_{\text{eval}}$ .

Then, we will show the interest of  $\mathcal{C}_{\text{eval}}$  when used together with other primitive contractors, in order to deal with general state observation functions such as Eq. (1b).

#### 3.1 Tube contractor for the constraint $\mathcal{L}_{\text{eval}} : z = y(t)$

Sometimes known as a *fleeting observation* [18], the constraint  $\mathcal{L}_{\text{eval}}$  differs from the ones presented in Section 2 that apply over the whole trajectory domain. Here, the evaluation leads to an improvement of the estimation of  $y(\cdot)$  around  $t$ . In a bounded error context, this constraint is defined by:

$$\mathcal{L}_{\text{eval}} : z = y(t), \quad t \in [t], z \in [z], y(\cdot) \in [y](\cdot). \quad (4)$$

The related contractor will aim at intersecting the tube by the envelope of all trajectories compliant with the bounded evaluation. In other words,  $[y](\cdot)$  will be contracted as the tube of all  $y(\cdot) \in [y](\cdot)$  going *through* the box  $[t] \times [z]$ , see Figure 4. Some trajectories may cross the box and leave it over  $[t]$ : the contractor must take into account this kind of propagation during the intersection process. To this end, the knowledge of the derivative  $\dot{y}(\cdot)$  is required to depict the evolution of  $y(\cdot)$ . In order to define the contractor in the most generic way, the derivative  $\dot{y}(\cdot)$  will be also bounded within a tube  $[w](\cdot)$ , thus allowing the  $[y](\cdot)$  contraction even if the derivative signal is uncertain.

The constraint  $\mathcal{L}_{\text{eval}}$  then amounts to the following CN:

$$\mathcal{L}_{\text{eval}} : \begin{cases} \text{Variables: } t, z, y(\cdot), w(\cdot) \\ \text{Constraints:} \\ (1) \quad z = y(t) \\ (2) \quad \dot{y}(\cdot) = w(\cdot) \\ \text{Domains: } [t], [z], [y](\cdot), [w](\cdot) \end{cases} \quad (5)$$

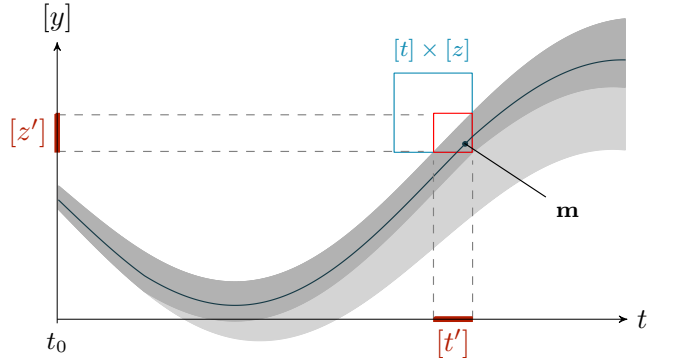


Fig. 4. Contraction of a tube  $[y](\cdot)$  from an evaluation constraint. A given measurement  $\mathbf{m} \in \mathbb{R}^2$ , pictured by a black dot, is known to belong to the blue box  $[t] \times [z]$ . The tube is contracted by means of  $\mathcal{C}_{\text{eval}}$ ; the contracted part is depicted in light gray. Meanwhile, the bounded observation itself is contracted to  $[t'] \times [z']$  with  $[t'] \subseteq [t]$  and  $[z'] \subseteq [z]$ . This is illustrated by the red box. The dark line is an example of a trajectory compliant with  $\mathbf{m}$ , enclosed within  $[t'] \times [z']$ .

**Proposition 2** A contractor  $\mathcal{C}_{eval}([t], [z], [y](\cdot), [w](\cdot))$  applying  $\mathcal{L}_{eval}$  on intervals and tubes is defined by:

$$\begin{pmatrix} [t] \\ [z] \\ [y](\cdot) \\ [w](\cdot) \end{pmatrix} \mapsto \begin{pmatrix} [t] \cap [y]^{-1}([z]) \\ [z] \cap [y]([t]) \\ [y](\cdot) \cap \bigsqcup_{t_1 \in [t]} \left( ([y](t_1) \cap [z]) + \int_{t_1}^{\cdot} [w](\tau) d\tau \right) \\ [w](\cdot) \end{pmatrix}. \quad (6)$$

**Proof.** To be a contractor,  $\mathcal{C}_{eval}$  needs to satisfy both the contraction and the consistency (i.e. no solution lost) properties from Definition 1. The contraction property is trivial as any variable is at least contracted by itself. Thus, it remains to prove that for two real numbers  $t \in [t]$ ,  $z \in [z]$  and two signals  $y(\cdot) \in [y](\cdot)$ ,  $w(\cdot) \in [w](\cdot)$  such that  $z = y(t)$ ,  $\dot{y}(\cdot) = w(\cdot)$ , we always have:

$$\begin{pmatrix} t \in [y]^{-1}([z]) & (i) \\ z \in [y]([t]) & (ii) \\ y(\cdot) \in \bigsqcup_{t_1 \in [t]} \left( ([y](t_1) \cap [z]) + \int_{t_1}^{\cdot} [w](\tau) d\tau \right) & (iii) \end{pmatrix}. \quad (7)$$

*Notation used hereafter:* considering a generic constraint  $\mathcal{L}_f : \mathbf{b} = \mathbf{f}(\mathbf{a})$ ,  $\mathbf{a} \in [\mathbf{a}]$ ,  $\mathbf{b} \in [\mathbf{b}]$ , the set  $\mathbb{B}$  of all vectors  $\mathbf{b}$  consistent with  $\mathcal{L}_f$  is  $[\mathbf{b}] \cap \bigcup_{\mathbf{a} \in [\mathbf{a}]} \mathbf{f}(\mathbf{a})$ . The closed and connected set enclosing  $\mathbb{B}$  and representable with intervals is  $\bigsqcup_{\mathbf{b} \in \mathbb{B}} = [\mathbf{b}] \cap \bigsqcup_{\mathbf{a} \in [\mathbf{a}]} \mathbf{f}(\mathbf{a})$  where the symbol  $\bigsqcup$  depicts the smallest envelope containing the following terms.

Proof of Eq. (7):

(i) the set  $\mathbb{T} \subset \mathbb{R}$  of all  $t$  consistent with  $\mathcal{L}_{eval}$  is:

$$\begin{aligned} \mathbb{T} &= [t] \cap \left( \bigcup_{y(\cdot) \in [y](\cdot)} \bigcup_{z \in [z]} y^{-1}(z) \right) \\ &\subset [t] \cap \left( \bigsqcup_{y(\cdot) \in [y](\cdot)} \bigsqcup_{z \in [z]} y^{-1}(z) \right) \\ &\subset [t] \cap [y]^{-1}([z]). \end{aligned}$$

An illustration of the evaluation of  $[y]^{-1}([z])$  is given in Figure 5.

(ii) the set  $\mathbb{Z} \subset \mathbb{R}$  of all  $z$  consistent with  $\mathcal{L}_{eval}$  is:

$$\begin{aligned} \mathbb{Z} &= [z] \cap \left( \bigcup_{y(\cdot) \in [y](\cdot)} \bigcup_{t \in [t]} y(t) \right) \\ &\subset [z] \cap \left( \bigsqcup_{y(\cdot) \in [y](\cdot)} \bigsqcup_{t \in [t]} y(t) \right) \\ &\subset [z] \cap [y]([t]). \end{aligned}$$

(iii) the value of  $y(t)$  from  $t_1$  is given by

$$y(t) = y_1 + \int_{t_1}^t w(\tau) d\tau, \quad \text{with } y_1 = y(t_1).$$

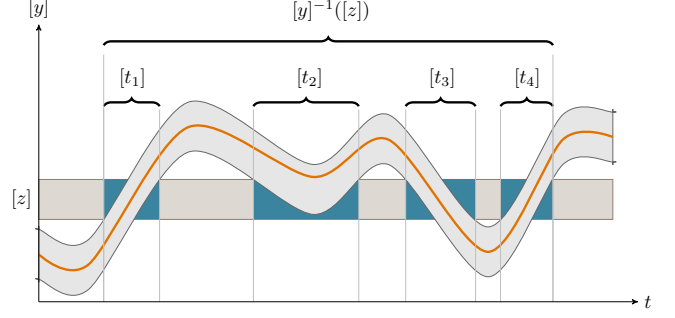


Fig. 5. Tube set-inversion  $[y]^{-1}([z])$ .  $[t_1]$ ,  $[t_2]$ ,  $[t_3]$ ,  $[t_4]$  are preimages subsets enclosed within the inversion result  $[y]^{-1}([z])$ .

The set  $\mathbb{Y} \subset \mathbb{R}$  of all  $y(t)$  consistent with  $\mathcal{L}_{eval}$  is:

$$\begin{aligned} \mathbb{Y} &= \bigcup_{t_1 \in [t]} \bigcup_{w(\cdot) \in [w](\cdot)} \bigcup_{y_1 \in [y](t_1) \cap [z]} \left( y_1 + \int_{t_1}^t w(\tau) d\tau \right) \\ &= \bigcup_{t_1 \in [t]} \left( \bigcup_{y_1 \in [y](t_1) \cap [z]} \left( y_1 + \bigcup_{w(\cdot) \in [w](\cdot)} \int_{t_1}^t w(\tau) d\tau \right) \right) \\ &= \bigcup_{t_1 \in [t]} \left( \left( \bigcup_{y_1 \in [y](t_1) \cap [z]} y_1 \right) + \int_{t_1}^t [w](\tau) d\tau \right) \\ &= \bigcup_{t_1 \in [t]} \left( ([y](t_1) \cap [z]) + \int_{t_1}^t [w](\tau) d\tau \right) \\ &\subset \bigsqcup_{t_1 \in [t]} \left( ([y](t_1) \cap [z]) + \int_{t_1}^t [w](\tau) d\tau \right). \quad \blacksquare \end{aligned}$$

The effect of  $\mathcal{C}_{eval}$  is highlighted in Figure 4 in a non-linear context and strong uncertainties. The derivative  $\dot{y}(\cdot)$ , not represented here, is also enclosed within a tube. Figure 6 pictures the result of an iterative process involving successive contractions.

One should note that the tube  $[y](\cdot)$  and both  $[t]$  and  $[z]$  may be contracted while the estimation of the derivative signal, represented by  $[w](\cdot)$ , will remain the same. Indeed, the evolution of any trajectory in  $[y](\cdot)$  cannot be known, except for degenerate tubes without thickness.

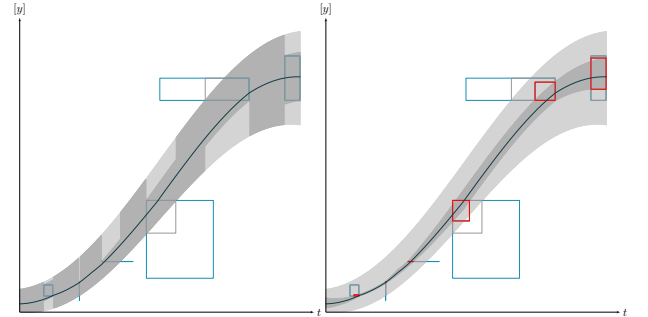


Fig. 6. Combined  $\mathcal{C}_{eval}$  contractions on a theoretical example involving a given tube  $[y](\cdot)$  and some measurements. The light gray part is the set of trajectories that have been removed after contractions. Blue boxes represent the initial measurements  $[t_i] \times [z_i]$ . Gray boxes picture intermediate contractions of these observations, obtained from the knowledge provided by the tube. Finally, red boxes depict the contracted measurements  $[t_i^*] \times [z_i^*]$  obtained after a fixed-point iterative method.

The derivative  $\dot{y}(\cdot) \in [w](\cdot)$  could then be of any arbitrary value. Therefore, no information from  $[y](\cdot)$  can be propagated back to  $[w](\cdot)$ . This is formalized and proved hereinafter.

**Lemma 3** Consider the constraint  $\dot{y}(\cdot) = w(\cdot)$  and two tubes  $[y](\cdot)$ ,  $[w](\cdot)$  such that there exists  $c(\cdot)$  differentiable and  $\varepsilon > 0$  with  $c(\cdot) + [-\varepsilon, \varepsilon] \subset [y](\cdot)$ . Then for all  $(w_1, t_1)$ , there exists a trajectory  $y(\cdot) \in [y](\cdot)$  such that  $\dot{y}(t_1) = w_1$ . As a consequence, no contraction can be expected for  $[w](\cdot)$  except in the cases of empty or degenerate tubes where  $[y](t)$  has no uncertainty for some consecutive times.

**Proof.** The function

$$a(t) = \frac{t}{1+t^2} \quad (8)$$

is inside the interval  $[-1, 1]$  and  $\dot{a}(0) = 1$ . Therefore, the function  $b(t) = \varepsilon a\left(\frac{\beta}{\varepsilon}(t - t_1)\right)$  is bounded by  $[-\varepsilon, \varepsilon]$  and

$$\dot{b}(t_1) = \varepsilon \frac{\beta}{\varepsilon} \dot{a}(0) = \beta. \quad (9)$$

We have

$$y(\cdot) = c(\cdot) + b(\cdot) \in [y](\cdot). \quad (10)$$

Thus,

$$\dot{y}(t_1) = \dot{c}(t_1) + \dot{b}(t_1) = \dot{c}(t_1) + \beta, \quad (11)$$

which is equal to  $w_1$  if we choose  $\beta = w_1 - \dot{c}(t_1)$ . As a consequence, for all  $(w_1, t_1)$ , there exists a consistent trajectory that belongs to  $[y](\cdot)$ . ■

**Domain of contraction.**  $\mathcal{C}_{\text{eval}}$  will propagate the constraint as much as possible over time in a forwards and backwards way. Contractions may cover the whole tube domain  $[t_0, t_f]$  or only a part of it, depending on the amount of uncertainties accumulated during the propagation. For instance in Figure 4, the contraction does not reach  $t_0$  in backwards.

**Inconsistency.** If the  $\mathcal{L}_{\text{eval}}$  constraint cannot be met over the domains  $[t]$ ,  $[z]$ ,  $[y](\cdot)$ ,  $[w](\cdot)$ , then  $\mathcal{C}_{\text{eval}}$  will perform a contraction to the empty set for  $[t]$ ,  $[z]$  and  $[y](\cdot)$ . This can be easily proved from Eq. (6).

**Multi-dimensions.** Extension to multi-dimensional problems  $\mathbf{z} = \mathbf{y}(t)$ ,  $\mathbf{z} \in \mathbb{R}^n$ ,  $\mathbf{y}(\cdot) \in \mathbb{R} \rightarrow \mathbb{R}^n$  amounts to applying  $\mathcal{L}_{\text{eval}}$  for each component  $z_j = y_j(t)$ ,  $j \in \{1 \dots n\}$ .

**Continuum of solutions over  $[t]$ .** The contractor also applies when several evaluations are bounded within the same  $([t], [z])$ , since the union of feasible trajectories

through any  $t \in [t]$  is kept after contraction. As an illustration, Figure 1 presents a case of three unknown evaluations enclosed within one bounded measurement  $([t], [\rho])$ .

**Set of evaluations.** When dealing with  $p \in \mathbb{N}$  evaluations, a single application of  $\mathcal{C}_{\text{eval}}$  for each  $([t_i], [z_i])$ ,  $i \in \{1 \dots p\}$  may not provide optimal results. Indeed,  $\mathcal{C}_{\text{eval}}$  propagates an evaluation along the whole domain of  $[y](\cdot)$  which may lead to new possible contractions. As pictured in Figure 6, it is preferable to use an iterative method that applies all contractors indefinitely until they become ineffective on  $[y](\cdot)$  and the  $([t_i], [z_i])$ 's:

$$\left( \bigcap_{i=1}^p \mathcal{C}_{\text{eval}}([t_i], [z_i], [y](\cdot), [w](\cdot)) \right)^\infty. \quad (12)$$

### 3.2 Application to state estimation

Let us come back to the state estimation problem this paper is dealing with. The classical state equations

$$\begin{cases} \dot{\mathbf{x}}(\cdot) = \mathbf{f}(\mathbf{x}(\cdot), \mathbf{u}(\cdot)), \\ z_i = g(\mathbf{x}(t_i)), \end{cases}$$

can be broken down into a set of primitive constraints, introducing variables  $\mathbf{v}(\cdot)$ ,  $y(\cdot)$  for ease of decomposition.

- (1)  $v_j(\cdot) = f_j(\mathbf{x}(\cdot), \mathbf{u}(\cdot))$
- (2)  $\dot{x}_j(\cdot) = v_j(\cdot)$ ,  $j \in \{1 \dots n\}$
- (3)  $y(\cdot) = g(\mathbf{x}(\cdot))$
- (4)  $z_i = y(t_i)$

Step (4) is the  $\mathcal{L}_{\text{eval}}$  constraint. In order to consider it, the derivative  $w(\cdot)$  of the *evaluated* trajectory  $y(\cdot)$  has to be defined:

- (1)  $v_j(\cdot) = f_j(\mathbf{x}(\cdot), \mathbf{u}(\cdot))$
- (2)  $\dot{x}_j(\cdot) = v_j(\cdot)$ ,  $j \in \{1 \dots n\}$
- (3)  $y(\cdot) = g(\mathbf{x}(\cdot))$
- (4)  $\mathcal{L}_{\text{eval}} : \begin{cases} z_i = y(t_i) \\ \dot{y}(\cdot) = w(\cdot) \end{cases}$
- (5)  $w(\cdot) = \dot{g}(\mathbf{x}(\cdot))$

Each constraint is then implemented by related primitive contractors. Domains will be reduced while keeping solutions compliant with the state equations. The differential contractor  $\mathcal{C}_{\frac{d}{dt}}$  introduced in [26] and the evaluation contractor  $\mathcal{C}_{\text{eval}}$  are respectively used for the above



steps (2) and (4). Algebraic constraints (1), (3), (5) are implemented with a composition of algebraic contractors on tubes such as  $\mathcal{C}_+$ ,  $\mathcal{C}_{\sin}$ ,  $\mathcal{C}_{\sqrt{\cdot}}$ , see Section 2.3.

- (1)  $\mathcal{C}_{f_j}([v_j](\cdot), [\mathbf{x}](\cdot), [\mathbf{u}](\cdot))$
- (2)  $\mathcal{C}_{\frac{d}{dt}}([x_j], [v_j]), j \in \{1 \dots n\}$
- (3)  $\mathcal{C}_g([y](\cdot), [\mathbf{x}](\cdot))$
- (4)  $\mathcal{C}_{\text{eval}}([t_i], [z_i], [y](\cdot), [w](\cdot))$
- (5)  $\mathcal{C}_{\dot{g}}([w](\cdot), [\mathbf{x}](\cdot))$

Set-membership state estimation then consists in an iterative process, each stage of which is calling these contractors. The process can be stopped when the tubes are not contracted anymore. One should note that the above contractors can be called in any order due to their monotonicity [2]. In this approach based on constraint propagations, the order can only impact the computation time: it could be more interesting to apply a contractor before another in order to perform the strongest contractions as soon as possible. However, this is highly specific to the considered problem.

Thus, the constraint satisfaction approach allows simplicity in the resolution of complex problems. This efficiency will be highlighted in the next sections presenting concrete applications. The proposed simulations are based on analytical expressions and simple data in order to encourage future comparisons with the method provided in this paper.

#### 4 Range-only robot localization involving low-cost beacons

Let us focus on a set-membership state estimation problem involving a robot  $\mathcal{R}$  moving amongst several beacons.

##### 4.1 Test case

The robot  $\mathcal{R}$  is described by its state  $\mathbf{x} \in \mathbb{R}^4$  where  $(x_1, x_2)$  depicts its location,  $x_3 = \psi$  its heading and  $x_4 = \vartheta$  its speed. The system is modeled by the following evolution function:

$$\begin{pmatrix} \dot{x}_1 \\ \dot{x}_2 \\ \dot{x}_3 = \dot{\psi} \\ \dot{x}_4 = \dot{\vartheta} \end{pmatrix} \xrightarrow{\mathbf{f}} \begin{pmatrix} \vartheta \cos(\psi) \\ \vartheta \sin(\psi) \\ u_1 \\ u_2 \end{pmatrix}. \quad (13)$$

Table 1  
Beacons' location and list of measurements  $([t_i], [z_i])$ .

$i$	$k$	$[t_i]$	$[z_i]$
1	$\beta$	[14.75, 15.55]	[11.69, 12.69]
2	$\alpha$	[20.80, 21.60]	[15.40, 16.40]
3	$\alpha$	[23.80, 24.60]	[10.62, 11.62]
4	$\alpha$	[26.80, 27.60]	[11.05, 12.05]
5	$\alpha$	[29.80, 30.60]	[11.87, 12.87]
6	$\alpha$	[32.80, 33.60]	[15.31, 16.31]
7	$\gamma$	[44.35, 45.15]	[13.65, 14.65]
8	$\gamma$	[47.35, 48.15]	[13.32, 14.32]
9	$\gamma$	[50.35, 51.15]	[12.03, 13.03]
10	$\gamma$	[53.35, 54.15]	[15.98, 16.98]
11	$\beta$	[56.75, 57.55]	[17.45, 18.45]

$k$	$\mathbf{b}_k$
$\alpha$	(30, 20)
$\beta$	(80, -5)
$\gamma$	(125, 20)

The state  $\mathbf{x}(t)$  is submitted to the input  $\mathbf{u}(t)$  whose value is bounded as:

$$\mathbf{u}(t) \in [\mathbf{u}](t) = \begin{pmatrix} -9/20 \cos(t/5) \\ 1/10 + \sin(t/4) \end{pmatrix} + \frac{1}{1000} \begin{pmatrix} [-1, 1] \\ [-1, 1] \end{pmatrix}. \quad (14)$$

The robot moves amongst low-cost beacons  $\mathbf{b}_k$ ,  $k \in \{\alpha, \beta, \gamma\}$ , thus implying drifting clocks (strong temporal uncertainties) and measurement errors. These emitters have a maximum signal range  $\rho_{\max} = 20\text{m}$  and send bounded signals  $z_i \in [z_i]$  on a regular basis with time uncertainties:  $t_i \in [t_i]$ . Then the observation function  $g_k$  (Eq. (1b)) related to a beacon  $\mathbf{b}_k$  is a distance function between  $\mathcal{R}$  and the beacon. The problem, also known as state estimation with *range-only* measurements [23, 7], will highlight the use of  $\mathcal{C}_{\text{eval}}$  based on a set of fleeing bounded measurements; see Table 1. Initial conditions are not known, except for  $\psi_0 \in \pi/2 + [-0.01, 0.01]$  and  $\vartheta_0 \in [-0.01, 0.01]$ . The simulation will be run from  $t_0 = 0$  to  $t_f = 64$ .

##### 4.2 Resolution

For ease of understanding, we will keep the same notations as in Section 3.2. The problem amounts to CN (15). The constraints form a network partially pictured in Figure 7 and are applied using contractors over intervals and tubes. Tubes are initialized to  $[-\infty, \infty] \forall t$  except for  $[\mathbf{u}](\cdot)$ , set according to Eq. (14). Furthermore in order to apply  $\mathcal{C}_{\text{eval}}$ , an estimation of the feasible derivatives of  $[y_k](\cdot)$ , represented by a tube  $[w_k](\cdot)$ , has to be computed. This is easily done analytically by deriving the distance function  $g_k$ .



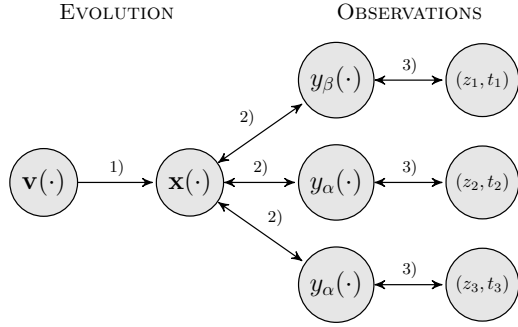


Fig. 7. Constraint network detailing the relations of the first three measurements of Table 1. Arrows indicate the possible directions of information propagation. For ease of understanding, derivatives  $w_k(\cdot)$  are not represented here.

**Variables:**

$\mathbf{x}(\cdot)$ ,  $\mathbf{v}(\cdot)$ ,  $\mathbf{u}(\cdot)$ ,  $\{(t_i, z_i)\}$ ,  $\{y_k(\cdot)\}$ ,  $\{w_k(\cdot)\}$

**Constraints:**

(1) Evolution function:

$$\begin{aligned} \mathbf{v}(\cdot) &= \mathbf{f}(\mathbf{x}(\cdot), \mathbf{u}(\cdot)) \\ \dot{\mathbf{x}}(\cdot) &= \mathbf{v}(\cdot) \\ x_3(0) &\in \pi/2 + [-0.01, 0.01] \\ x_4(0) &\in [-0.01, 0.01] \end{aligned}$$

(2) Observation function:

$$\begin{aligned} y_k(\cdot) &= \sqrt{(x_1(\cdot) - b_{k,1})^2 + (x_2(\cdot) - b_{k,2})^2} \\ w_k(\cdot) &= \frac{(x_1(\cdot) - b_{k,1}) \cdot v_1(\cdot) + (x_2(\cdot) - b_{k,2}) \cdot v_2(\cdot)}{\sqrt{(x_1(\cdot) - b_{k,1})^2 + (x_2(\cdot) - b_{k,2})^2}} \\ \dot{y}_k(\cdot) &= w_k(\cdot) \end{aligned}$$

(3) Measurements:

$$z_i = y_k(t_i)$$

**Domains:**

$[\mathbf{x}](\cdot)$ ,  $[\mathbf{v}](\cdot)$ ,  $[\mathbf{u}](\cdot)$ ,  $\{[t_i], [z_i]\}$ ,  $\{[y_k](\cdot)\}$ ,  $\{[w_k](\cdot)\}$

(15)

Then the process involving contractors, explained in Section 3.2, is executed. The fixed point is reached over 52 iterations in 2 minutes, but the main contractions are already obtained before the sixth iteration, as pictured in Figure 8: the position domain is slightly reduced during the next steps. A projection of the computed results is pictured in Figure 9. This example shows how the constraint satisfaction approach behaves: in an iterative way and without a necessary knowledge on the initial conditions. At the end, the true state trajectory  $\mathbf{x}^*(\cdot)$  is guaranteed to lie within the tube  $[\mathbf{x}](\cdot)$ .

**Remark 4** Results could be improved by bisecting the state space. Indeed, several states  $\mathbf{x}(t_i) \in [\mathbf{x}](t_i)$  may lead to the same observation  $z_i = g(\mathbf{x}(t_i))$  since function  $g$  is not injective. Then, bisections can help to consider independently several states consistent with the observation, and reject them if not consistent with the other constraints.

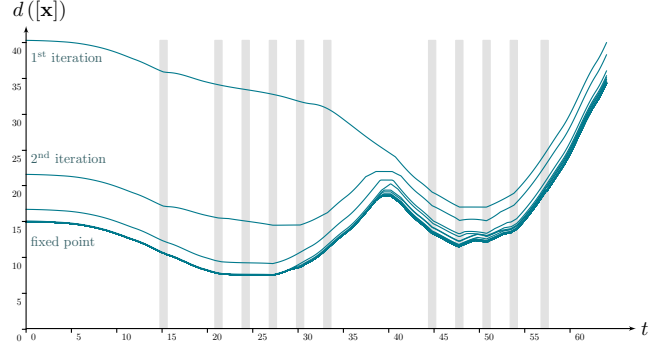


Fig. 8. Thicknesses of the position estimation  $[x_1](\cdot) \times [x_2](\cdot)$  for each iteration step. We define  $d : \mathbb{R}^2 \rightarrow \mathbb{R}$  the diagonal of a position box  $[x_1] \times [x_2]$ :  $d([\mathbf{x}]) = \sqrt{(x_1^+ - x_1^-)^2 + (x_2^+ - x_2^-)^2}$ . This depicts in the worst case the error between the unknown truth and any trajectory within the tube. Uncertain measurements' times  $[t_i]$  are projected in light gray. The fixed point has been reached after 52 iterations while almost final results were already obtained during the first steps.

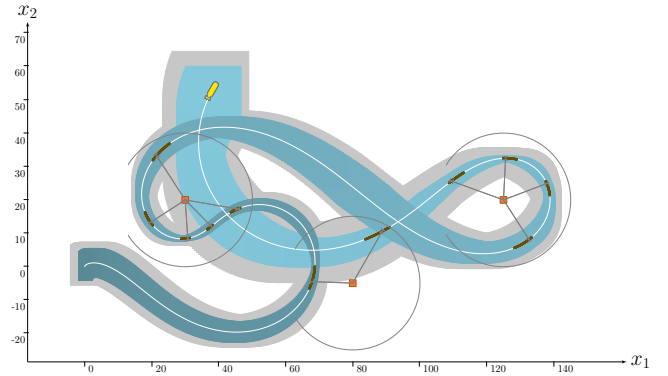


Fig. 9. State estimation of a mobile robot among a set of beacons, as detailed in Section 4. The initial position  $(0, 0)$  is not known. Beacons, pictured by red boxes, are sending signals till a range limit depicted by circles. Time uncertainties  $[t_i]$  are projected along the robot path with dark thick lines. The true poses of the robot are pictured by the white line, enclosed within the estimated tubes  $[x_1](\cdot) \times [x_2](\cdot)$  projected in blue and gray. The pessimism induced by time uncertainties is represented in light gray. In other words, the blue part depicts a state estimation assuming a precise knowledge on the  $t_i$ 's.

## 5 Reliable correction of a drifting clock

A complementary illustration of this work is the situation of a drifting clock: an isolated clock that does not run at the same rate as a reference clock. This problem amounts to increasing time uncertainties that can be reduced using a collaborative method.

### 5.1 Test case

An underwater system, lying on the seabed at  $(0, 0, -10)$ , is equipped with a low-cost drifting clock. Absolute

time reference is represented by  $t$  while the time value  $\tau$  provided by the underwater clock is drifting<sup>1</sup> such that:

$$\tau = h(t) = 0.045t^2 + 0.98t. \quad (16)$$

However, this information is not known: the problem consists in estimating this function. Instead, we shall assume the following bounded derivative of  $h(\cdot)$ , that could be obtained from the clock data-sheet:

$$\dot{h}(t) \in [0.08, 0.12] \cdot t + [0.97, 1.08]. \quad (17)$$

The problem is constrained thanks to a localized robot  $\mathcal{B}$  evolving at the surface and a set of measured distances  $z_i \in \mathbb{R}$  between the robot and the underwater clock, see Figure 10 and Table 2. The boat's trajectory  $\mathbf{x}(\cdot) : \mathbb{R} \rightarrow \mathbb{R}^2$  is preprogrammed, forming a kind of ephemeris for the clock in the same way as stars have been used for celestial navigation on Earth. This way, the beacon already knows where the robot must be at time  $t$ . Conversely, detecting the location of  $\mathcal{B}$  provides a temporal information to be compared with the embedded time value. Hence, the boat can be used by the underwater clock to correct this temporal drift.

However, the boat may not precisely respect the defined schedule. The ephemeris thus consists in a tube  $[\mathbf{x}(\cdot)]$  taking into account the possible error of the boat location. The velocity  $\mathbf{v}(\cdot)$  of  $\mathcal{B}$  is also bounded:

$$\mathbf{x}(\cdot) \in \begin{pmatrix} [70, 90] \\ [10, 30] \end{pmatrix} + 100 \begin{pmatrix} \cos(\cdot) \\ \sin(\cdot) \end{pmatrix}, \quad (18)$$

$$\mathbf{v}(\cdot) \in \begin{pmatrix} [-0.1, 0.1] \\ [-0.1, 0.1] \end{pmatrix} + 100 \begin{pmatrix} -\sin(\cdot) \\ \cos(\cdot) \end{pmatrix}. \quad (19)$$

<sup>1</sup> In order to keep things simple in this academic example, we consider that the clock perfectly matches the absolute time reference at  $t = 0$ :  $h(0) = 0$ . But any unknown offset could be assumed with our resolution method.

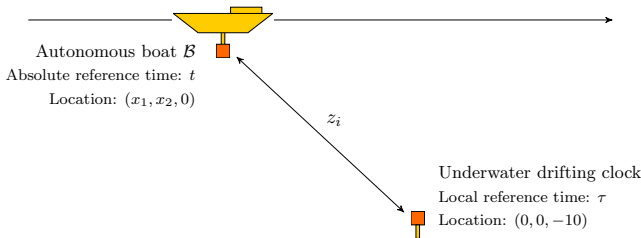


Fig. 10. Illustrating the problem of a drifting clock corrected by ephemerides provided by an autonomous boat  $\mathcal{B}$ . The beacon holding the clock receives distance measurements from the boat once in a while.

## 5.2 Resolution

The problem amounts to the following CN (20). The same notations are used as in Section 3.2. Function  $y(\cdot)$  now depicts the prevision of the distances separating the boat from the beacon. Each measurement is referenced by  $\tau_i$  that are temporal drifting values given by the underwater clock. The estimation of  $h(\cdot)$ , depicting the drift and bounded within a tube  $[h](\cdot)$ , will provide a reliable enclosure of the reference time  $t_i$  corresponding to each  $\tau_i$ :  $t_i \in [h]^{-1}(\tau_i)$ . The measurements values  $z_i$  are now referenced by  $([t_i], [z_i])$  and will then be constrained by  $y(\cdot)$  through  $\mathcal{L}_{\text{eval}}$ . In particular, the estimation  $[t_i]$  will be refined. Another  $\mathcal{L}_{\text{eval}}$  will constrain the  $h(\cdot)$  trajectory, based on the temporal pairs  $([t_i], \tau_i)$ . To this end, the derivative of  $h(\cdot)$ , denoted  $\phi(\cdot)$  and bounded by Eq. (17), will be considered too.

As before, contractors are called on tubes in place of constraints on trajectories listed in CN (20). Tubes  $[\mathbf{x}(\cdot)]$ ,  $[\mathbf{v}(\cdot)]$ ,  $[\phi(\cdot)]$  are respectively initialized according to Equations (18), (19) and (17). This time, the contractor of interest  $\mathcal{C}_{\text{eval}}$  will be called twice, see Constraints (4) of CN (20).

}	<b>Variables:</b>	$\{(t_i, z_i)\}, \mathbf{x}(\cdot), \mathbf{v}(\cdot), h(\cdot), \phi(\cdot), y(\cdot), w(\cdot)$
	<b>Constraints:</b>	
	(1) Ephemerides ( <i>i.e.</i> boat locations):	$\dot{\mathbf{x}}(\cdot) = \mathbf{v}(\cdot)$
	(2) Beacon-boat distance function:	$y(\cdot) = \sqrt{x_1(\cdot)^2 + x_2(\cdot)^2 + (-10)^2}$ $w_k(\cdot) = (x_1(\cdot) \cdot v_1(\cdot) + x_2(\cdot) \cdot v_2(\cdot)) / y(\cdot)$ $\dot{y}_k(\cdot) = w_k(\cdot)$
(3) Drifting time function:	$\dot{h}(\cdot) = \phi(\cdot)$ $h(0) = 0$	
(4) Measurements:	$z_i = y(t_i)$ $\tau_i = h(t_i)$	
<b>Domains:</b>	$\{([t_i], [z_i])\}, [\mathbf{x}(\cdot)], [\mathbf{v}(\cdot)], [h](\cdot), [\phi](\cdot), [y](\cdot), [w](\cdot)$	

Tube inversions on  $[h](\cdot)$  provide the corresponding enclosures  $[t_i] = [h]^{-1}(\tau_i)$  of absolute reference times  $t_i$ , see Figure 12. The  $[t_i]$  are then used to read the ephemeris and are contracted by:

$$([t_i], [z_i], [y](\cdot), [w](\cdot)) \xrightarrow{\mathcal{C}_{\text{eval}}} ([t_i], [z_i], [y](\cdot), [w](\cdot)). \quad (21)$$

Table 2

List of measurements  $(\tau_i, [z_i])$ .

$i$	$\tau_i$	$[z_i]$
1	1.57	[152.47, 156.47]
2	3.34	[34.67, 38.67]
3	5.32	[102.38, 106.38]
4	7.50	[184.45, 188.45]
5	9.88	[167.09, 171.09]
6	12.46	[60.03, 64.03]
7	15.25	[78.76, 82.76]
8	18.24	[175.88, 179.88]

The contracted  $[t_i]$  can then be used to reduce the tube  $[h](\cdot)$  using the same contractor:

$$([t_i], \tau_i, [h](\cdot), [\phi](\cdot)) \xrightarrow{C_{\text{eval}}} ([t_i], \tau_i, [h](\cdot), [\phi](\cdot)). \quad (22)$$

An iterative resolution process is executed up to a fixed point. Indeed, the first contraction of  $[h](\cdot)$  (Eq. (22))

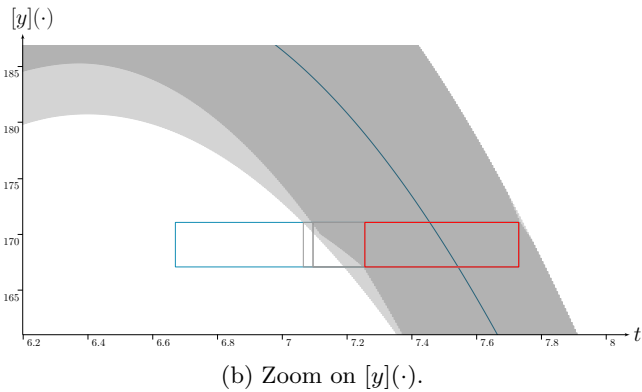
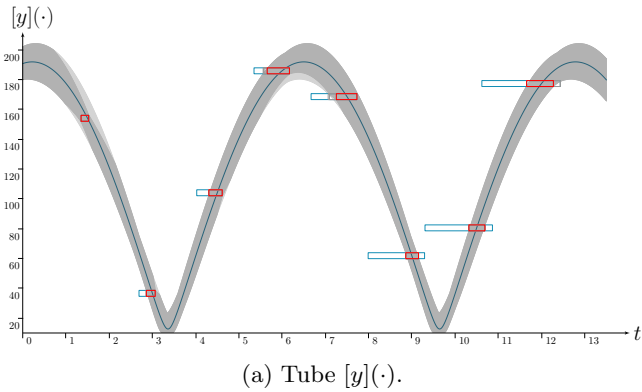


Fig. 11. Tube  $[y](\cdot)$  representing the reliable prevision of the distances between the boat and the beacon (so-called *ephemeris*).  $[y](\cdot)$  is submitted to a set of measurements pictured by blue boxes, before their final contraction in red. This demonstrates the contraction of strong time uncertainties by  $C_{\text{eval}}$  thanks to the knowledge provided by the tube itself.

raises new constraints for the contraction of the  $[t_i]$  (Eq. (21)). In this example, constraints have been propagated over 5 steps of computation in less than 2 seconds.

Finally, the contracted tube  $[h](\cdot)$  reflects the clock drift correction, see Figure 12. We emphasize that the real drift  $h(t)$ , unknown of the resolution, remains enclosed in its final envelope  $[h](t), \forall t$ .

## 6 Conclusions

This paper provides an original method to deal with time uncertainties in non-linear and differential systems. The proposed framework, based on tubes depicting envelopes of trajectories, is generic, reliable and simple to use. The principle is to model the problem as a constraint network and generate a contractor from each constraint. The tubes containing the variables are then contracted as much as possible. The main added value of this paper is to provide an elementary contractor to deal with trajectory evaluations in a bounded error context, while considering any uncertainty on these variables.

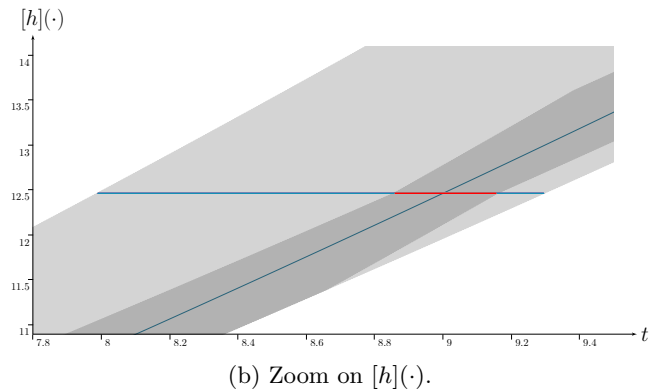
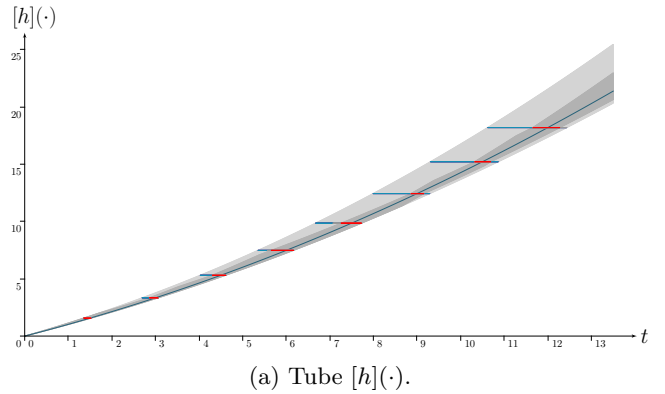


Fig. 12. Tube  $[h](\cdot)$  representing the clock drift. For a given time  $\tau_i$ ,  $[h]^{-1}(\tau_i)$  provides an enclosure  $[t_i]$  of the time reference  $t_i$ . When  $[t_i]$  is contracted by means of ephemeris  $[y](\cdot)$  and  $C_{\text{eval}}$  (see Figure 11), the information can be propagated back to  $[h](\cdot)$ . The tube's contracted part is pictured in light gray while the real drift expressed by Eq. (16) is plotted in blue.

From a practical standpoint, this contractor now also allows to consider state estimation problems from a temporal point of view [25], where the time  $t$  becomes an unknown variable to be estimated. This new approach, here introduced over simple examples of mobile robotics, opens the way to further applications in which the consideration of time uncertainties is relevant. The obtained solutions are guaranteed and can be used for proof purposes, *e.g.* algorithm validations, path planning, collision avoidance or formal verification of robot behavior.

## 7 Available libraries

The *Tubex* library implemented during this work and the source code of the simulated examples presented in this paper are available on [www.simon-rohou.fr/research/tubeval](http://www.simon-rohou.fr/research/tubeval). This framework is compatible with *IBEX*: a C++ library for system solving and global optimization based on interval arithmetic and constraint programming, see [www.ibex-lib.org](http://www.ibex-lib.org). Figures have been drawn using the visualizer VIBEs [12].

## Acknowledgements

This work has been supported by the French *Direction Générale de l'Armement* (DGA) during the UK-France PhD program.

## References

- [1] J. Alexandre dit Sandretto and A. Chapoutot. “Validated Explicit and Implicit Runge-Kutta Methods”. In: *Reliable Computing electronic edition*. Special issue devoted to material presented at SWIM 2015 22 (July 2016).
- [2] K. R. Apt. “The essence of constraint propagation”. In: *Theoretical Computer Science* 221.1 (June 28, 1999), pp. 179–210.
- [3] I. Araya, G. Trombettoni, and B. Neveu. “A Contractor Based on Convex Interval Taylor”. In: *Integration of AI and OR Techniques in Constraint Programming for Combinatorial Optimization Problems: 9th International Conference, CPAIOR 2012, Nantes, France, May 28 – June 1, 2012. Proceedings*. Ed. by N. Beldiceanu, N. Jussien, and É. Pinson. Berlin, Heidelberg: Springer Berlin Heidelberg, 2012, pp. 1–16.
- [4] C. Bessiere. “Constraint Propagation”. In: *Foundations of Artificial Intelligence*. Ed. by F. Rossi, P. van Beek, and T. Walsh. Vol. 2. Supplement C vols. Handbook of Constraint Programming. Elsevier, Jan. 1, 2006, pp. 29–83.
- [5] A. Bethencourt and L. Jaulin. “Cooperative localization of underwater robots with unsynchronized clocks”. In: *Paladyn, Journal of Behavioral Robotics* 4.4 (Jan. 27, 2013).
- [6] A. Bethencourt and L. Jaulin. “Solving Non-Linear Constraint Satisfaction Problems Involving Time-Dependant Functions”. In: *Mathematics in Computer Science* 8.3 (Sept. 2014), pp. 503–523.
- [7] J. L. Blanco, J. Gonzalez, and J. A. Fernandez-Madrigal. “A pure probabilistic approach to range-only SLAM”. In: 2008 IEEE International Conference on Robotics and Automation. May 2008, pp. 1436–1441.
- [8] G. Chabert and L. Jaulin. “Contractor programming”. In: *Artificial Intelligence* 173.11 (July 1, 2009), pp. 1079–1100.
- [9] M. Choi, J. Choi, J. Park, and W. K. Chung. “State estimation with delayed measurements considering uncertainty of time delay”. In: 2009 IEEE International Conference on Robotics and Automation. May 2009, pp. 3987–3992.
- [10] C. Combastel. “A State Bounding Observer for Uncertain Non-linear Continuous-time Systems based on Zonotopes”. In: IEEE Conference on Decision and Control. 2005, pp. 7228–7234.
- [11] B. Desrochers and L. Jaulin. “A minimal contractor for the polar equation: Application to robot localization”. In: *Engineering Applications of Artificial Intelligence* 55 (Supplement C Oct. 1, 2016), pp. 83–92.
- [12] V. Drevelle and J. Nicola. “VIBes: A Visualizer for Intervals and Boxes”. In: *Mathematics in Computer Science* 8.3 (Sept. 2014), pp. 563–572.
- [13] T. F. Filippova, A. B. Kurzhanski, K. Sugimoto, and I. Vályi. “Ellipsoidal State Estimation for Uncertain Dynamical Systems”. In: *Bounding Approaches to System Identification*. Ed. by M. Milanese, J. Norton, H. Piet-Lahanier, and É. Walter. Boston, MA: Springer US, 1996, pp. 213–238.
- [14] A. Gning and P. Bonnifait. “Constraints propagation techniques on intervals for a guaranteed localization using redundant data”. In: *Automatica* 42.7 (July 1, 2006), pp. 1167–1175.
- [15] L. Jaulin, M. Kieffer, I. Braems, and E. Walter. “Guaranteed non-linear estimation using constraint propagation on sets”. In: *International Journal of Control* 74.18 (Jan. 2001), pp. 1772–1782.
- [16] L. Jaulin, M. Kieffer, O. Didrit, and É. Walter. *Applied Interval Analysis*. London: Springer London, 2001.

- [17] A. B. Kurzhanski and T. F. Filippova. “On the Theory of Trajectory Tubes — A Mathematical Formalism for Uncertain Dynamics, Viability and Control”. In: *Advances in Nonlinear Dynamics and Control: A Report from Russia*. Ed. by A. B. Kurzhanski. Boston, MA: Birkhäuser Boston, 1993, pp. 122–188.
- [18] F. Le Bars, J. Sliwka, L. Jaulin, and O. Reynet. “Set-membership state estimation with fleeting data”. In: *Automatica* 48.2 (Feb. 2012), pp. 381–387.
- [19] A. K. Mackworth. “Consistency in Networks of Relations”. In: *Artif. Intell.* 8.1 (Feb. 1977), pp. 99–118.
- [20] M. Milanese and A. Vicino. “Estimation theory for nonlinear models and set membership uncertainty”. In: *Automatica* 27.2 (Mar. 1, 1991), pp. 403–408.
- [21] R. Moore. *Interval analysis*. Prentice-Hall series in automatic computation. Prentice-Hall, 1966.
- [22] R. Moore. *Methods and Applications of Interval Analysis*. Studies in Applied and Numerical Mathematics. Society for Industrial and Applied Mathematics, 1979.
- [23] P. Newman and J. Leonard. “Pure range-only sub-sea SLAM”. In: 2003 IEEE International Conference on Robotics and Automation (Cat. No.03CH37422). Vol. 2. Sept. 2003, 1921–1926 vol.2.
- [24] T. Raïssi, N. Ramdani, and Y. Candau. “Set membership state and parameter estimation for systems described by nonlinear differential equations”. In: *Automatica* 40.10 (Oct. 1, 2004), pp. 1771–1777.
- [25] S. Rohou. “Reliable robot localization: a constraint-programming approach over dynamical systems”. PhD thesis. Brest, France: Université de Bretagne Occidentale, Dec. 2017.
- [26] S. Rohou, L. Jaulin, L. Mihaylova, F. Le Bars, and S. M. Veres. “Guaranteed computation of robot trajectories”. In: *Robotics and Autonomous Systems* 93 (2017), pp. 76–84.
- [27] P. Van Hentenryck, L. Michel, and F. Benhamou. “Constraint programming over nonlinear constraints”. In: *Science of Computer Programming. Concurrent Constraint Programming* 30.1 (Jan. 1, 1998), pp. 83–118.
- [28] D. Wilczak, P. Zgliczyński, P. Pilarczyk, M. Mrozek, T. Kapela, Z. Galias, J. Cyranka, and M. Capinski. *Computer Assisted Proofs in Dynamics group, a C++ package for rigorous numerics*. <http://capd.ii.uj.edu.pl>. 2017.